CLOSED-FORM SOLUTION OF A METAL PLATE WITH A CENTRAL CRACK UNDER TENSION

Ali Ehsan Seif and Mohammad Zaman Kabir[*]

Department of Civil Engineering, Amirkabir University of Technology (Tehran Polytechnic), Hafez Street, Tehran, Iran
e-mail: seyf@aut.ac.ir, mzkabir@aut.ac.ir
*corresponding author

Abstract

Accurate prediction of stress and displacement in plates with central cracks is vital for engineering design safety. However, the impact of finite plate size on stress and displacement distribution is an important factor that has not been fully addressed in previous studies, highlighting the need for further investigation. Thus, this study presents a closed-form elastic solution for a rectangular plate with a central crack under tension load. The solution uses complex polynomial functions satisfying equilibrium equations and boundary conditions. Numerical finite element models verify the analytical solution's accuracy for plates with varying crack lengths. The presented closed-form solution accounts for the impact of finite plate size on stress and displacement distribution accurately. Developing closed-form solutions for structural mechanics problems enables engineers to optimize designs for safety, efficiency, and cost-effectiveness more accurately.

Keywords: Finite cracked plate, size effect, closed-form solution, stress prediction.

1. Introduction

While an elastic solution for the crack problem in an infinite medium is readily available in many references (Sadd, 2005), closed-form solutions for real problems with limited sizes have not been provided due to the complexity of applying boundary conditions. Despite this limitation, the stress intensity factor in finite bodies has been studied extensively by researchers to consider size restrictions at the crack-tip fields.

In the review paper by Isida (1971), a collocation method was employed to apply boundary conditions to a cracked strip under uniform tension, resulting in the estimation of the crack-tip stress intensity factor, while Wu et al. (1983, 1984, 1989) used the weight function method to calculate stress intensity in finite bodies under arbitrary loading conditions, a technique that has since been widely adopted by researchers such as Rice (1972), Fet (1999), Ng and Lau (1999), Kiciak et al. (2003), and Jones et al. (2004). Other methods used to estimate stress intensity factors in finite plates with multiple cracks include the general method presented by Cheung et al. (1992) and the Eigen function method used by Jun and Yu-qiu (1992), while more recent paper by Chen (2011) utilized the superposition of the Zener-Stroh crack problem in an infinite plate and a usual Griffith crack problem in a finite plate to calculate stress intensity factors.

Various studies have utilized numerical methods to investigate crack-tip fields in finite bodies under different loading conditions, alongside analytical works. Among these methods, the finite element method is widely used and has been employed by several researchers, including Rybicki and Kanninen (1977) and Guangwei et al. (1998). Additionally, Vafai and Estekanchi (1999) conducted a thorough examination of the stress and displacement fields in cracked plates and shells using finite element models. Palani et al. (2008) combined the crack closure technique with finite element models to determine the strain energy release rate and stress intensity factor. Nevertheless, other numerical methods have been used, as demonstrated by Rangelova et al. (2003) and Sahli et al. (2007), who evaluated the stress intensity factor using two different boundary element numerical methods.

Numerous studies in the existing literature on the crack problem have focused on specific geometries or boundary conditions, providing numerical values of the stress intensity factor or empirical relations for the associated correction factor (Kabir and Aghdam 2019; 2021). However, Vafai and Estekanchi (1999) conducted an exceptional study using the numerical approach of finite element analysis to evaluate all stress and displacement fields in an entire cracked plate. Analytically, Seif and Kabir (2015, 2016) obtained the general form of stress and displacement fields, as well as the buckling load of symmetric and anti-symmetric modes for finite cracked plates. Subsequently, in their papers (2017, 2018), they verified the analytical results of buckling loads with experimental data by testing both modes under monotonic and fatigue cyclic loads, studying the effect of buckling on fracture capacity and fatigue life. In their more recent paper (2019), Seif and Kabir utilized the spline finite strip method to model the nonlinear post-buckling state and provided analytical approaches to evaluate the fracture capacity and fatigue life of notched sheets in the presence of buckling.

The primary objective of the present study is to build upon the previous research conducted by Seif and Kabir in 2016, which explored the analytical form of stress and displacement fields in finite cracked plates. In order to achieve this, we aim to present a closed-form solution that takes into consideration the equilibrium equations and boundary conditions, with the aim of determining the unknown coefficients. To achieve this objective, the paper provides a detailed overview of the elastic fields' general form before delving into the method of analytical development. This approach allows us to present a comprehensive and robust analytical solution that takes into account all the necessary variables and parameters. Moreover, the paper aims to verify the validity of the analytical relations by comparing them with numerical results obtained using the finite element method. This will help establish the accuracy and precision of the analytical solution presented. Overall, the study represents a significant contribution to the field of finite cracked plates, as it presents a novel and more efficient approach to the determination of the stress and displacement fields. It is hoped that the results of this study will be useful in the design and analysis of structures that rely on finite cracked plates.

2. Analytical approach

2.1. General forms of the elastic fields

Seif and Kabir (2016) presented a comprehensive solution for the elastic stress and displacement fields of a cracked plate depicted in Fig. 1. This solution is applicable to both finite and infinite cracked plates. To obtain the solution, the authors utilized the potential functions of infinite cracked plates and expanded them around the crack-tip. Consequently, the obtained results comprise infinite series forms of stresses and displacements. It is worth noting that the solution does not consider the plate's shape and boundary conditions. The presented solution is considered general, as the coefficients of the infinite series were not determined analytically, leading to an unknown value for these coefficients.
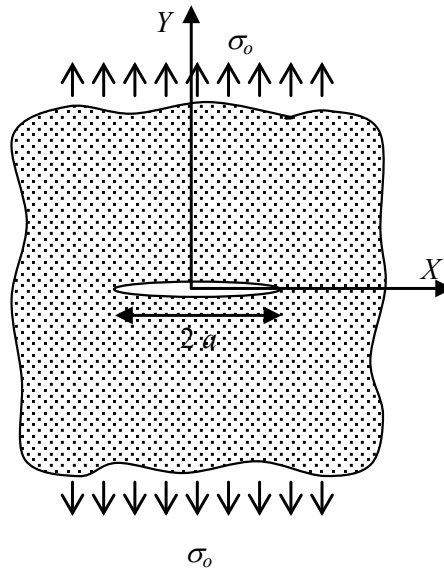
Fig. 18. Central cracked plate under tension.

We take into consideration the complex form of the fundamental elastic relations for the stress and displacement fields as the basis for our solution.

$$\sigma_{yy} + \sigma_{xx} = 2\left(\gamma' + \overline{\gamma}'\right) \tag{1}$$

$$\sigma_{yy} - \sigma_{xx} + 2i\tau_{xy} = 2\left(\overline{Z}\gamma'' + \psi'\right) \tag{2}$$

$$2\mu(U + iV) = k\gamma - Z\overline{\gamma}' - \overline{\psi} \tag{3}$$

where $Z = X + iY$ is the well-known coordinate in the complex domain with the definition of $i = \sqrt{-1}$, γ and ψ are the complex potential functions, μ and k are defined in terms of the elasticity modulus E and Poisson's ratio v as $\mu = E/2(1+v)$ and $k = (3-v)/(1+v)$ and the prime and over-bar signs denote the derivative with respect to Z and the complex conjugate, respectively. A comparison between the general forms and the classic relation for infinite cracked plates is illustrated in Figure 2.

<div align="center">

Classic relations of infinite cracked plates   **General relations for both finite and infinite cracked plates**

</div>

$$\gamma = \frac{\sigma_o}{4}\left(2\sqrt{Z^2-a^2}-Z\right)$$

$$\gamma = \frac{\sigma_o}{4}\left[\sum_{n=0}^{\infty}2A_n(Z^2-a^2)^{n+1/2}-B_0 Z\right]$$

$$\psi = \frac{\sigma_o}{2}\left(Z-\frac{a^2}{\sqrt{Z^2-a^2}}\right)$$

$$\psi = \frac{\sigma_o}{2}\left[B_0 Z-\sum_{n=0}^{\infty}a^2 A_n(Z^2-a^2)^{n-1/2}\right]$$

$$\sigma_{xx} = \sigma_o\,\mathrm{Re}\left[\frac{2Z(Z^2-a^2)-a^2(Z-\overline{Z})}{2\left(\sqrt{Z^2-a^2}\right)^3}-1\right]$$

$$\sigma_{xx} = \frac{\sigma_o}{2}\,\mathrm{Re}\left\{\sum_{n=0}^{\infty}A_n H_n\left[2Z^2(Z-n\overline{Z})-a^2\left(\left(\frac{2n+3}{2n+1}\right)Z-\overline{Z}\right)\right]\right\}-B_0\sigma_o$$
*

$$\sigma_{yy} = \sigma_o\,\mathrm{Re}\left[\frac{2Z(Z^2-a^2)+a^2(Z-\overline{Z})}{2\left(\sqrt{Z^2-a^2}\right)^3}\right]$$

$$\sigma_{yy} = \frac{\sigma_o}{2}\,\mathrm{Re}\left\{\sum_{n=0}^{\infty}A_n H_n\left[2Z^2(Z+n\overline{Z})-a^2\left(\left(\frac{6n+1}{2n+1}\right)Z+\overline{Z}\right)\right]\right\}$$
*

$$\tau_{xy} = \sigma_o\,\mathrm{Im}\left[\frac{a^2(Z-\overline{Z})}{2\left(\sqrt{Z^2-a^2}\right)^3}\right]$$

$$\tau_{xy} = \frac{\sigma_o}{2}\,\mathrm{Im}\left\{\sum_{n=0}^{\infty}A_n H_n\left[2Z^2(n\overline{Z})-a^2\left(\left(\frac{2n-1}{2n+1}\right)Z+\overline{Z}\right)\right]\right\}$$
*

$$U = \frac{\sigma_o}{4\mu}\,\mathrm{Re}\left[\frac{a^2-Z\overline{Z}}{\sqrt{\overline{Z}^2-a^2}}+k\sqrt{Z^2-a^2}+(\frac{1-k}{2})Z-\overline{Z}\right]$$ $$U = \frac{\sigma_o}{4\mu}\,\mathrm{Re}\left\{\sum_{n=0}^{\infty}A_n J_n-B_0\left[(\frac{k-1}{2})Z+\overline{Z}\right]\right\}$$ **

$$V = \frac{\sigma_o}{4\mu}\,\mathrm{Im}\left[\frac{a^2-Z\overline{Z}}{\sqrt{\overline{Z}^2-a^2}}+k\sqrt{Z^2-a^2}+(\frac{1-k}{2})Z-\overline{Z}\right]$$ $$V = \frac{\sigma_o}{4\mu}\,\mathrm{Im}\left\{\sum_{n=0}^{\infty}A_n J_n-B_0\left[(\frac{k-1}{2})Z+\overline{Z}\right]\right\}$$ **

$$*\,H_n = (2n+1)(Z^2-a^2)^{n-3/2},\qquad **\,J_n = k(Z^2-a^2)^{n+1/2}-\left[(2n+1)Z\overline{Z}-a^2\right]\left(\overline{Z}^2-a^2\right)^{n-1/2}$$

**Fig. 19.** Elastic stresses and displacements of the cracked plate (Seif and Kabir, 2016)

2.2. Closed-Form Solution

On the right-hand side of Figure 2, the complex series represent the extended elastic relations from an infinite cracked plate to a finite one. Nevertheless, these series comprise an infinite number of terms with unknown coefficients, which can only describe the general form of stresses and displacements, irrespective of the plate's shape and boundary conditions. The objective of this section is to derive a closed-form solution for a rectangular, tensioned finite plate with a central crack, as depicted in Figure 3.
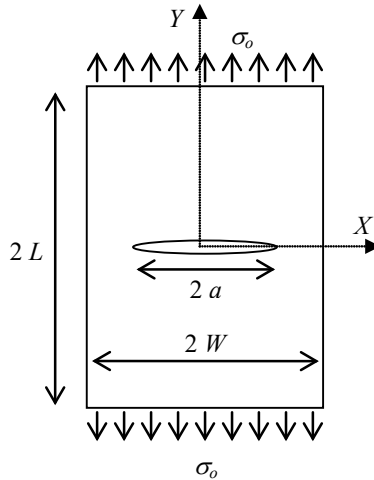
Fig. 20. A finite plate with a central cracked under applied tension.

In order to obtain a closed-form solution for the problem, it is necessary to determine the unknown coefficients Ai and Bi on the right-hand side of Figure 2. These coefficients can be mathematically derived from the equilibrium equations and boundary conditions. However, since the number of such relations is limited, only a finite number of coefficients can be derived. Therefore, the number of terms in the analytical solution is proportional to the number of available relations. To take advantage of the symmetry of the problem, we consider a quarter of the plate, as depicted in Figure 4.
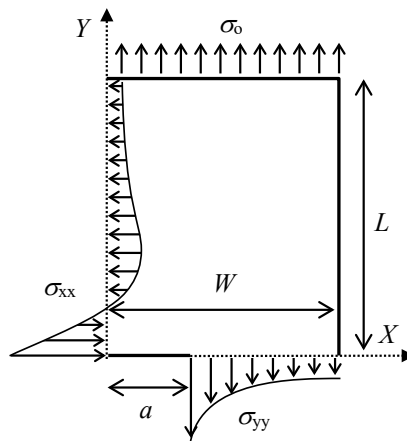
Fig. 21. Schematic stress distribution in a quarter of a cracked plate.

The model illustrated in Figure 4 leads to a force equilibrium in the X and Y directions, given by:

$$\int_0^L \sigma_{xx}(0,Y)\, dY = 0 \qquad (4)$$

$$\int_a^W \sigma_{yy}(X,0)\, dX = \sigma_o \times W \tag{5}$$

Furthermore, the boundary conditions of stress and displacement can be considered as defined relations. The potential functions γ and ψ are naturally compatible with the symmetry of the problem and the boundary conditions associated to the symmetry of the problem, including the stresses and displacements on the axes of X and Y, do not give new relations. Therefore, the stress conditions on the outer edges of the plate, $X = W$ and $Y = L$ are considered as

$$\sigma_{xx}(W,0) = 0 \tag{6}$$

$$\sigma_{yy}(0,L) = \sigma_o \tag{7}$$

By utilizing the last four relations, we can determine the four unknowns, which include a single parameter, B_o, and three coefficients, A_o, A_1, and A_2, corresponding to the first three terms of the infinite series. By considering the first three terms from the relations on the right-hand side of Figure 2, we can simplify the normalized stress profiles as follows:

$$\sigma_{xx}(0,Y)=\sigma_o\left\{A_o\left[\frac{Y(2a^2+Y^2)}{(\sqrt{a^2+Y^2})^3}\right]+A_1\left[\frac{-2Y(2a^2+3Y^2)}{\sqrt{a^2+Y^2}}\right]+A_2\left[3Y\sqrt{a^2+Y^2}\,(3a^2+5Y^2)\right]-B_o\right\} \tag{8}$$

$$\sigma_{yy}(0,Y)=\sigma_o\left\{A_o\left[\frac{Y^3}{(\sqrt{a^2+Y^2})^3}\right]+A_1\left[\frac{-2Ya^2}{\sqrt{a^2+Y^2}}\right]+A_2\left[Y\sqrt{a^2+Y^2}\,(4a^2-5Y^2)\right]\right\} \tag{9}$$

$$\sigma_{xx}(X,0)=\sigma_o\left\{A_o\left[\frac{X}{\sqrt{X^2-a^2}}\right]+A_1\left[\frac{-a^2X}{\sqrt{X^2-a^2}}\right]+A_2\left[-X\sqrt{X^2-a^2}\,(5X^2+a^2)\right]-B_o\right\} \tag{10}$$

$$\sigma_{yy}(X,0)=\sigma_o\left\{A_o\left[\frac{X}{\sqrt{X^2-a^2}}\right]+A_1\left[\frac{X(6X^2-5a^2)}{\sqrt{X^2-a^2}}\right]+A_2\left[3X\sqrt{X^2-a^2}\,(5X^2-3a^2)\right]\right\} \tag{11}$$

Substituting (eq. 8-11) into (eq. .4-7), four unknown coefficients A_o, A_1, A_2 and B_o are determined in terms of geometry characteristics of the rectangular cracked plate W, L and a. The obtained results for a square plate with different crack lengths are tabulated in Table 1.

a/W	B_o	A_o	A_1	A_2
0.20	1.0817	1.0600	-0.0008	0.0000003
0.25	1.1291	1.0937	-0.0020	0.0000020
0.30	1.1888	1.1349	-0.0042	0.0000090
0.35	1.2617	1.1836	-0.0079	0.0000319
0.40	1.3497	1.2397	-0.0137	0.0000967
0.45	1.4551	1.3035	-0.0223	0.0002600
0.50	1.5813	1.3751	-0.0345	0.0006380

Table 1. The results obtained for a square plate with various crack lengths.

By plugging the derived coefficients into the first three terms of the series shown on the right-hand side of Figure 2, we can determine the elastic stress and displacement fields over the entire

cracked plate. To illustrate, Figure 5 displays the stress distribution obtained for a square cracked plate with a/W = 0.35, in comparison to the infinite cracked plate.
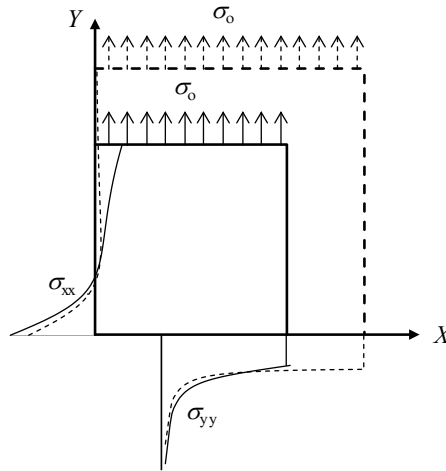

Fig. 22. The stress distribution is depicted by the solid line for the quarter of the square cracked plate with finite sizes, whereas the dashed line corresponds to the infinite ones.

As shown in Figure 5, the stress distribution in the cracked plate is notably affected by the finite size of the plate. Specifically, the singular stress intensity at the crack-tip of the finite plate, denoted by σ_{yy}, is higher when compared to that of the infinite cracked plate. In fracture mechanics, such an intensification of stress at the crack tip is defined by the well-known correction factor β. In the case of σ_{xx}, a similar increase appears at the crack edge and unexpectedly at the upper edge of the plate. However, the profile of stress σ_{xx} in both finite and infinite cracked plates coincide nearly at the zero point of stress (see Figure 5). It should be noted that the current solution considers only three terms of the series. As a result, the method presented provides an approximate closed-form solution for the elastic stresses and displacements of the finite cracked plates. To verify the accuracy of the current solution, a parametric study and numerical modeling, such as the finite element method, are required, which will be discussed in the following section.

## 3. Numerical modelling and verifications

To validate the closed-form solution presented, a numerical finite element method was employed using the ABAQUS software. The numerical models were constructed using 4-node doubly curved general-purpose shell elements S4R. Similar to the analytical approach, only a quarter of a square sheet was modelled due to the biaxial symmetry of the plate, with overall dimensions of 200 mm width and a half crack length of a = 70 mm. After conducting sensitivity analysis, the mesh divisions of the model were determined, as shown in Figure 6, with refinement near the crack tip. In comparison, the analytical results of the closed-form solution were calculated at uniform intervals of 5 mm in both the X and Y directions.
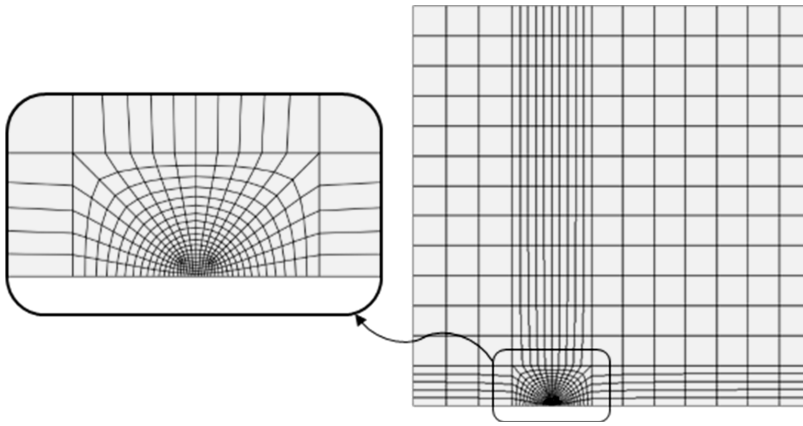
Fig. 23. Mesh layout for finite element analysis.

The stress and displacement results of the closed-form solution and finite element method (FEM) were obtained under a uniform tension stress of 100 MPa. As the presented closed-form solution is the first of its kind for cracked plates with limited dimensions, contour plots were used to display the results. Figures 7 and 8 depict the comparison between the stress and displacement contours obtained from the closed-form solution and the numerical FEM simulations. The results show that the quality and quantity of the closed-form solution are in acceptable agreement with the numerical results of the finite element method.
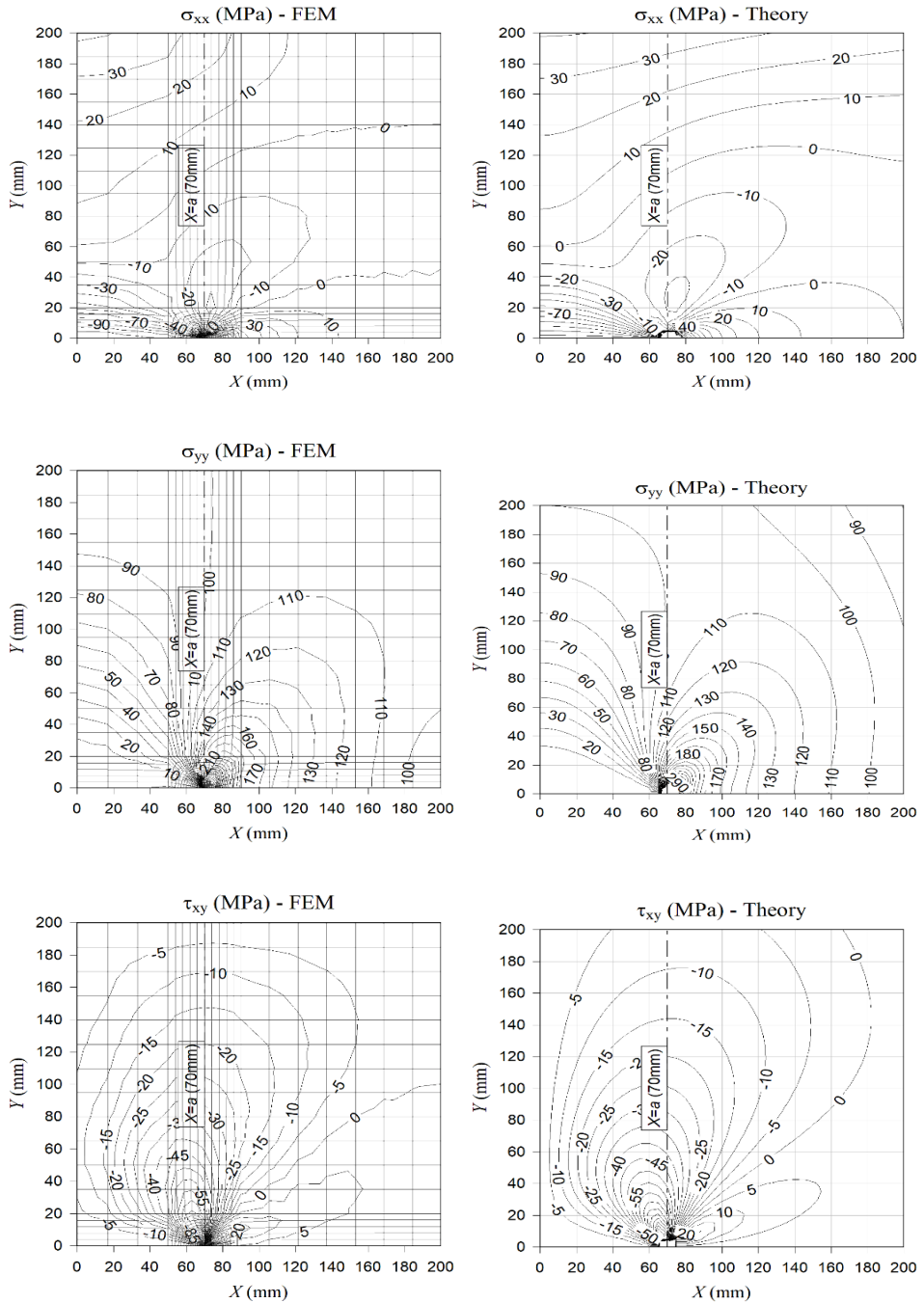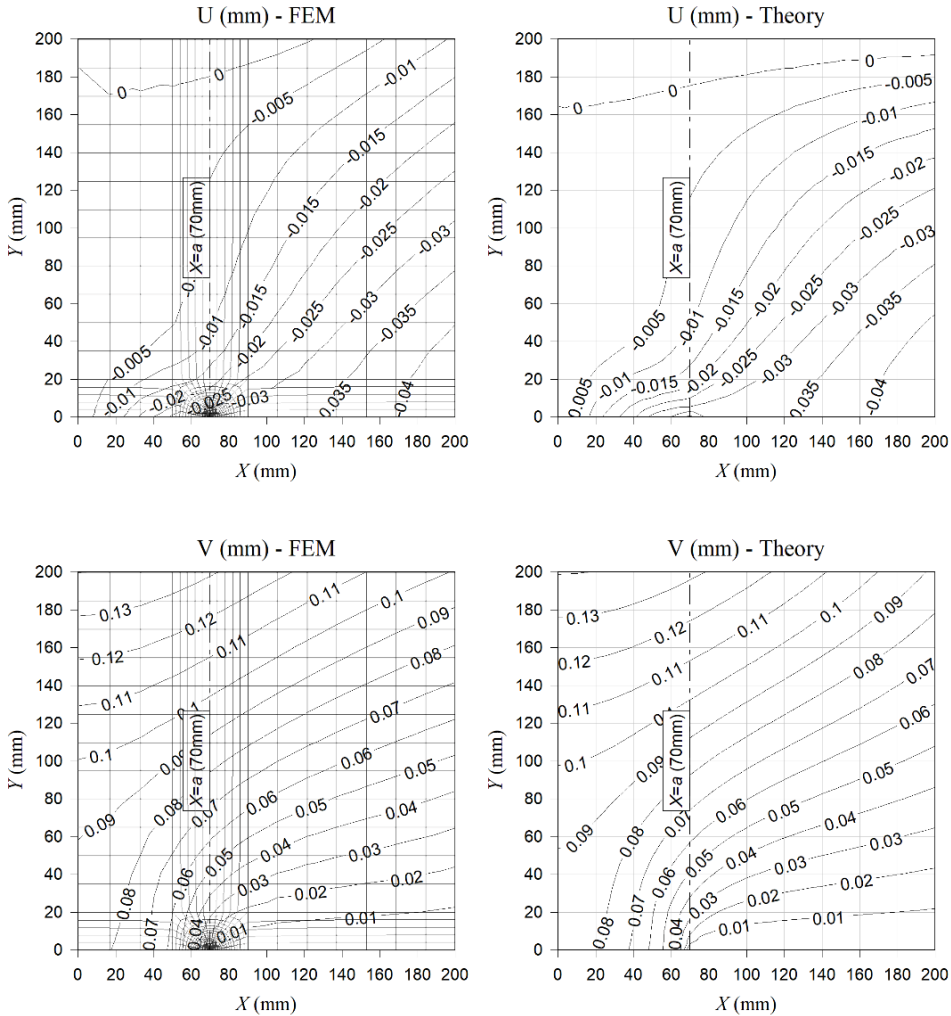
Fig. 24. Comparison between the closed-form solution (Theory) and numerical finite element method (FEM) results for in-plane stress fields.

Based on Figure 7, it can be observed that both numerical and analytical results show similar stress distributions around the crack tip, as well as the pattern of remote stresses. This indicates that the presented closed-form solution considers the singularity of the crack-tip stress and also

takes into account the effects of exterior boundary conditions. Displacement contour plots in Figure 8 also show good agreement between numerical and analytical results. These contours are more uniform compared to the stress contours, as there is no singularity condition in the displacement fields. In conclusion, the comparison made in Figures 7 and 8 suggests that the analytical relations on the right-hand side of Figure 2, with the factors tabulated in Table 1, accurately provide the elastic fields of stress and displacement throughout the entire finite cracked plate.


Fig. 25. Comparison between the numerical results of the in-plane displacement fields obtained from the finite element method (FEM) and the closed-form solution (Theory).

To perform a thorough examination, stress and displacement diagrams along the X and Y axes were obtained from both the finite element method and the presented closed-form solution. Three different crack lengths, $a/W = 0.2$, 0.35, and 0.5, were considered small, medium, and large cracks. In addition, the classical solution of the infinite cracked plate (relations on the left-hand side of Figure 2) was included to emphasize the effect of finite sizes considered by the current

closed-form solution, which can also be taken as the theoretical lower limit of the relative crack length (e.g. a/W ≈ 0). The combined effects of crack length and plate size are briefly referred to as the size effect. The normalized stress and displacement diagrams are shown in Figures 9-12.

Figure 9 illustrates the normalized diagrams of stresses, denoted as σ_{xx} and σ_{yy}, through the X-axis (where Y = 0) for various crack lengths. Results obtained using both the finite element method and the closed-form solution demonstrate that stresses near the crack tip are significantly intensified due to the size effect, which is known to increase as the crack widens. The stress diagram for σ_{xx} approaches zero at the free edge of the plate (a = W), as described by equation (6) in the closed-form solution. Conversely, the stress diagram for σ_{yy} has a non-zero value at the plate edge, which decreases as the crack length progresses. This is explained by equation (5), which states that the total area under the σ_{yy} diagram remains constant, independent of the crack length. Consequently, the stress value on one side of the diagram is diminished as the crack-tip stress on the other side increases, maintaining the total area constantly. Overall, the results obtained using the closed-form solution and numerical finite element simulations are in reasonable agreement, as demonstrated in Figure 9. This agreement is also evident in Figure 10, which shows that the general form of displacement diagrams is unaffected by the size effect.
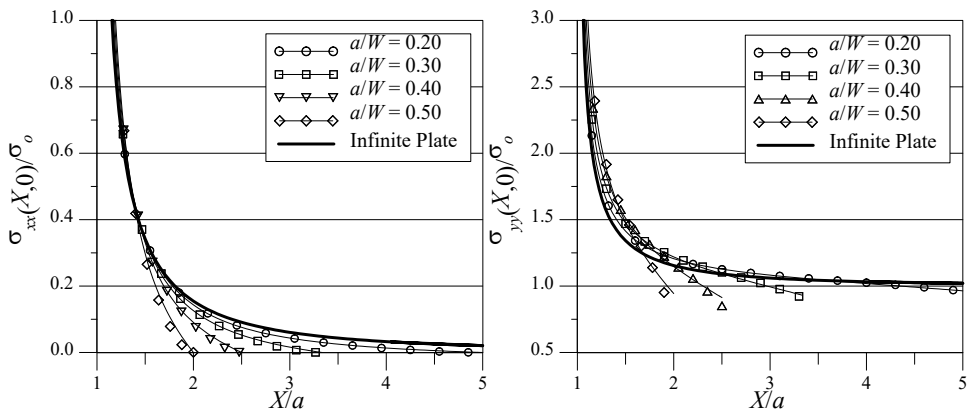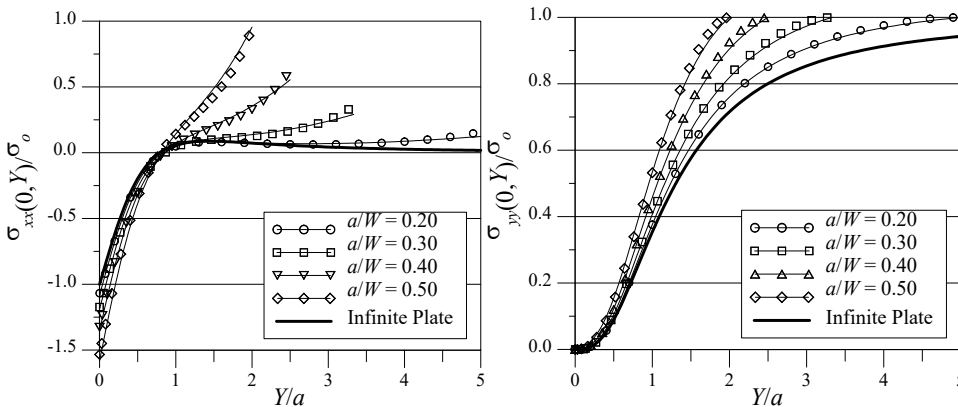

Fig. 26. The stress diagrams normalized at Y = 0 and X ≥ a are depicted using symbols for the finite element method, thin lines for the current closed-form solution of a finite cracked plate, and a bold line for the classic theory of an infinite cracked plate.
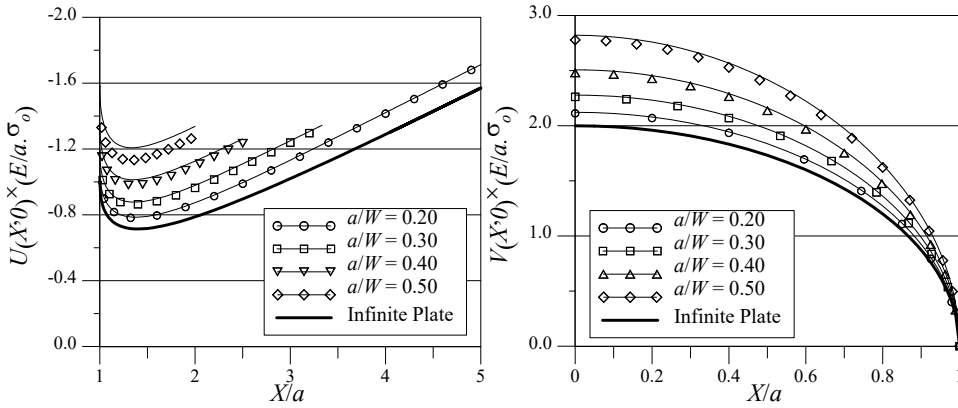
Fig. 27. The normalized displacement diagrams at Y = 0 are shown using symbols for the finite element method, thin lines for the current closed-form solution of a finite cracked plate, and a bold line for the classic theory of an infinite cracked plate.

Normalized stress diagrams through the Y axis (X=0) are depicted in Figure 11. As the crack grows, both numerical and analytical results indicate that the maximum compressive stress is amplified for σ_{xx}. To account for this increase in compressive stress due to the size effect, Seif and Kabir (2015) introduced a new correction factor, denoted as β'. Moreover, the finite element results demonstrate that changes in tensile stress are more significant. The stress diagram generally exhibits a descending trend within the tensile phase for the infinite cracked plate, while for the finite cracked plates, it unexpectedly rises. This difference is also well established by the closed-form solution. Theoretical equation (4) asserts that the total area beneath the tensile stress diagram is in equilibrium with that of the compressive stress. Thus, to fulfil the equilibrium equation (4), increasing the maximum compressive stress because of size limitation must also lead to an increase in tensile stress (Kabir and Hooton (2020), Kabir et al. (2020)).

Fig. 28. At X=0, the stress diagrams are normalized and obtained from three sources: the finite element method (represented by symbols), the current closed-form solution of the finite cracked plate (represented by thin lines), and the classic theory of infinite cracked plate (represented by a bold line).

All stress diagrams for σ_{yy} depict a zero-stress value at the free edge of the crack (Y=0). Furthermore, according to equation (7), the stress value should achieve the remote stress σ_o at the loading edge of the plate (Y=L). This fact is evident from both the finite element method and the closed-form solution prediction, as shown in Figure 11. In regard to σ_{yy} and the vertical displacement V in Figure 12, the impact of finite size on the overall trend of the diagrams is considered insignificant. In other words, the finite size effect can only be observed as an increase in stress and displacement linked to the improvement in relative crack length.
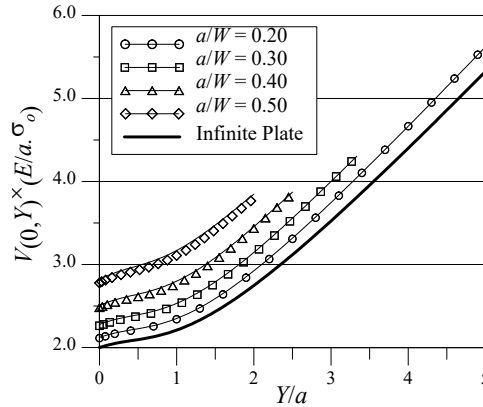
Fig. 29. At X=0, the displacement diagrams are normalized and obtained from three sources: finite element method (represented by symbols), the current closed-form solution of the finite cracked plate (represented by thin lines), and the classic theory of infinite cracked plate (represented by a bold line).

It is evident from Figures 9 to 12 that the size effect can substantially alter the shape of the stress and displacement diagrams. The impact of the size effect is more prominent in plates with wider cracks, particularly near the boundaries. Nevertheless, the current solution effectively accounts for the size effect in the finite cracked plates, and the resulting outcomes are in excellent agreement with the numerical results.

4. Conclusion

In this paper, we reviewed the general form of elastic fields in finite cracked plates previously presented by the authors and compared it with the conventional solution to the crack problem in an infinite plate. We discussed the relevant boundary conditions in a rectangular plate with a central crack, as well as the equilibrium equations in the quarter model of the plate. This resulted in four relations associated with two stress boundary conditions and two force equilibriums. Finally, we provided a closed-form solution for the finite cracked plate by taking the first three terms from the existing general solution and applying the four known relations. We presented the number of coefficients for a square plate with various crack lengths and verified the obtained elastic fields with the results of the finite element method made in the ABAQUS environment. The contour plots in a cracked plate with a/W = 0.35 showed the excellent conformity of the current closed-form solution with the numerical results of the finite element method over the entire plate.

Based on the stress contour plots, we concluded that the presented closed-form solution accurately reflects the singularity of the crack-tip stress and the effects of outer boundary

conditions. For the displacement fields, analytical and numerical contours are more compatible due to the lack of singularity. We obtained normalized diagrams of the elastic stress and displacement fields in a square plate with relatively small, medium, and large cracks from the current closed-form solution and compared them with the numerical results of the finite element method. The diagrams showed how the stress and displacement diagrams change due to the size effect, with more changes observed over the plates with wider cracks. The major change in the form of the diagram was found in the case of σ_{xx} through the Y axis. Our results exhibited that the presented closed-form solution recognizes all size effects in finite cracked plates and is in good agreement with the numerical results. In conclusion, the presented closed-form solution for the elastic fields in finite cracked plates is an accurate and useful tool for engineers and researchers studying the behavior of cracked plates in various applications.

References

Chen Y.Z. (2011). Zener-Stroh Crack Problem in a Finite Plate. Journal of Marine Science and Technology, 19, 2, 127-131

Cheung Y.K., Woo C.W. and Wang Y.H. (1992). A general method for multiple crack problems in a finite plate, Computational Mechanics, 10, 5, 335-343.

Fett T. (1999). Stress intensity factors for edge-cracked plates under arbitrary loading. Fatigue & fracture of engineering materials & structures, 22, 4, 301-305

Guangwei M., Suhuan C., Hanbing L. and Zhichao W. (1998). The influence of plate size with double cracks on stress intensity factor. Communications in numerical methods in engineering, 14, 5, 429-436

Isida M. (1971). Effect of width and length on stress intensity factors of internally cracked plates under various boundary conditions, International Journal of Fracture Mechanics, 7, 3, 301-316

Jones R., Peng D., Pitt S. and Wallbrink C. (2004). Weight functions, CTOD, and related solutions for cracks at notches, Engineering Failure Analysis, 11, 1, 79–114

Jun Q. and Yu-qiu L. (1992). The expression of stress and strain at the tip of notch in Reissner plate. Applied Mathematics and Mechanics, 13, 4, 315-324

Kabir, H. and Aghdam, M. M. (2019). A robust Bézier based solution for nonlinear vibration and post-buckling of random checkerboard graphene nano-platelets reinforced composite beams. Composite Structures, 212, 184-198.

Kabir, H. and Hooton, R. D. (2020). Evaluating soundness of concrete containing shrinkage-compensating MgO admixtures. Construction and Building Materials, 253, 119141.

Kabir, H., Hooton, R. D. and Popoff, N. J. (2020). Evaluation of cement soundness using the ASTM C151 autoclave expansion test. Cement and Concrete Research, 136, 106159.

Kabir, H. and Aghdam, M. M. (2021). A generalized 2D Bézier-based solution for stress analysis of notched epoxy resin plates reinforced with graphene nanoplatelets. Thin-Walled Structures, 169, 108484.

Kiciak A., Glinka G. and Burns D.J. (2003). Calculation of Stress Intensity Factors and Crack Opening Displacements for Cracks Subjected to Complex stress Fields, Journal of Pressure Vessel Technology, 125, 3, 260-266

Ng S.W. and Lau K.J. (1999). A new weight function expression for through cracks, Engineering Fracture Mechanics, 64, 5, 515-537

Palani G.S., Iyer N.R. and Dattaguru B. (2006). A generalised technique for fracture analysis of cracked plates under combined tensile, bending and shear loads. Computers & structures, 84, 29-30, 2050-2064

Rangelova T., Dinevab P. and Gross D. (2003). A hyper-singular traction boundary integral equation method for stress intensity factor computation in a finite cracked body, Engineering Analysis with Boundary Elements, 27, 1, 9–21

Rybicki E.F. and Kanninen M.F. (1977). A finite element calculation of stress intensity factors by a modified crack closure integral, Engineering fracture mechanics, 9, 4, 931-938

Rice J.R. (1972). Some remarks on elastic crack-tip stress fields, International Journal of Solids and Structures, 8, 6, 751-758

Sadd M.H. (2005). Elasticity: Theory, Applications and Numerics, Elsevier Inc, Oxford

Sahli A., Boutchicha D., Belarbi A. and Rahmani O. (2007). Stress intensity solutions for cracked plates by the dual boundary method, Strength of Materials, 39, 5, 513-522

Seif A.E. and Kabir M.Z. (2015). An efficient analytical model to evaluate the first two local buckling modes of finite cracked plate under tension. Latin American Journal of Solids and Structures, 12, 11, 2078-2093

Seif A.E. and Kabir M.Z. (2016). The general form of the elastic stress and displacement fields of the finite cracked plate, Journal of Theoretical and Applied Mechanics, 54, 4, 1271-1283

Seif A.E. and Kabir M.Z. (2017). Experimental Study on the Fracture Capacity and Fatigue Life Reduction of the Tensioned Cracked Plate due to the Local Buckling, Engineering fracture Mechanics, 175, 168–183

Seif A.E. and Kabir M.Z. (2018). Innovative fixture for the buckling measurements of the notched plates under monotonic and cyclic tensile loading, Experimental Techniques, 42, 4, 371–382

Seif A.E. and Kabir M.Z. (2019). Spline finite strip modelling of post-buckling behaviour in the notched tensioned sheets considering analytical approaches for fracture and fatigue, Thin-Wallled Strucures, 137, 541-560

Vafai A. and Estekanchi H.E. (1999). A parametric finite element study of cracked plates and shells. Thin-Walled Structures, 33, 3, 211-229

Wu X.R. and Carlsson J. (1983). The generalised weight function method for crack problems with mixed boundary conditions, Journal of The Mechanics and Physics of Solids, 31, 6, 485-497

Wu X.R. (1984). Approximate weight functions for center and edge cracks in finite bodies, Engineering Fracture Mechanics, 20, 1, 35-49

Wu X.R. and Chen X.G. (1989). Wide-range weight function for center cracks, Engineering Fracture Mechanics, 33, 6, 877-886